Arch. Mech., 36, 2, pp. 219–232, Warszawa 1984

Large-angle cone-shaped bodies in supersonic three-dimensional stream(*)

P. I. CHUSHKIN (MOSCOW)

THE NUMERICAL investigation of three-dimensional flow about large-angle cone-shaped bodies at an angle of attack in supersonic free stream of gas is carried out. The bodies have a finite length, a small bluntness at the apex and an angle exceeding the limiting one. The mixed flow behind the detached shock wave is calculated by the method of integral relations using the special variables which are consistent with the flow behaviour near the body apex. The influence of the free stream parameters and the body geometry is studied. Both cones and cone-shaped concave noses are considered.

Przeprowadzono obliczenia numeryczne dotyczące trójwymiarowego opływu szerokokątowych ciał stożkowych pod kątem natarcia w ponaddźwiękowym strumieniu swobodnym gazu. Ciała mają skończoną długość i wierzchołki o zatępieniu przekraczającym wartość graniczną. Przepływ za oderwaną falą uderzeniową analizuje się za pomocą związków całkowych, stosując specjalne zmienne zgodnie z charakterem przepływu w pobliżu wierzchołka. Zbadano wpływ parametrów strumienia swobodnego i geometrii ciała. Rozważono zarówno przypadki stożków jak również wklęsłych dysz stożkowych.

Проводится численное исследование трехмерного обтекания конусовидных тел с большим углом раствора, расположенных под углом атаки в сверхзвуковом потоке газа. Тела имеют конечную длину, малое затупление у вершины и угол раствора, превышающий предельный. Смешанное течение за отошедшей ударной волной рассчитывается методом интегральных соотношений в специальных переменных, учитывающих поведение течения у вершины тела. Изучено влияние параметров невозмущенного потока и геометрии тела. Рассмотрены как конусы, так и конусовидные вогнутые носовые части.

1. Introduction

WE CONSIDER cone-shaped bodies having a semi-angle greater than its limiting value and located in a supersonic free stream of an ideal gas at an angle of attack. In this case, even if the body apex has a small bluntness, an arising detached shock wave is mainly determined by the body sides rather than by the bluntness. The mixed subsonic-supersonic rotational flow about the body, which is essentially three-dimensional in the case under consideration, can be calculated with the help of numerical methods only. An analogous situation takes place for an arbitrary pointed body with a sufficiently large apex semi-angle.

Computations of flows about cones with large apex angles and large bluntnesses have been successfully carried out by a number of authors who used different numerical techniques such as the finite-difference method, the net-characteristics method, the method of lines. Information on works of this kind can be found in the survey by VOSKRESENSKY and CHUSHKIN [1].

(*) Paper given at XVI Symposium on Advanced Problems and Methods in Fluid Mechanics, Spała, 4–10 September, 1983.

But let us take a different case. If a large-angle conical body has a sharp apex or a small apex bluntness (with a curvature radius smaller than 1% of the body length), serious computational difficulties occur. The fact is that the tip is a singular point with any standard coordinates and here derivatives of gasdynamical functions are infinite (even in the case of zero angle of attack), while near a small bluntness they are limited but very great. The situation becomes more complicated for three-dimensional flows.

Owing to these difficulties, only few works devoted to computations of three-dimensional flows about pointed nose parts of bodies with detached shock wave have been published. For this case IVANOVA and RADVOGIN [2, 3] adapted the well-known finite-difference method proposed by BABENKO and VOSKRESENSKY [4], but these authors confined themselves only to small angles of attack. KOVENYA, TARNAVSKII and YANENKO [5] developed a technique of splitting up by which a flow about a pointed body at small angle of attack was calculated as an example, but here the body tip was not strictly treated and was actually cut off. The laborious unsteady three-dimensional methods were used in these two papers, and the time-asymptotic solutions were computed.

The simple and reasonable solution of the problem under consideration was calculated using the method of integral relations proposed by DORODNICYN [6]. Having introduced some special coordinates which take into account the singularity at the body tip, CHUSHKIN [7] for the first time obtained reliable results by this method for symmetric flows past sharp cones and wedges with semi-angles within the wide interval from the limiting values to those exceeding 90°. Later the author extended his approach to the case of the angle of attack and considered wedges [8] and axisymmetrical cones [9] with small apex bluntnesses and finite lengths.

In the present paper the author wishes to continue this numerical investigation of three-dimensional flows about large-angle conical bodies with a detached shock wave at a supersonic free stream velocity. Here some new results are reported for bodies with a smaller bluntness radius and for flow regimes closer to the limiting ones. Besides, the generalization of the method to the case of bodies with noncircular (elliptical) cross-section is described.

2. Governing equations and boundary conditions

Let us to consider flows about cone-shaped bodies located at an angle of attack in a supersonic free stream with the Mach number M_∞. The gas is supposed to be inviscid non-heatconducting and perfect with the constant specific heat ratio $\varkappa$. The body has a semi-angle ω exceeding its limiting value ω_{lim}, a small apex bluntness and a given finite length limited by the base with the sonic shoulder.

The spherical system of coordinates r, θ, ψ is initially taken (Fig. 1), in which $\psi = 0$ and $\psi = \pi$ correspond to the leeward and windward planes, respectively. Owing to the flow symmetry, the region of interest is bounded by the meridional planes $\psi = 0$ and $\psi = \pi$. To take into account the behaviour of flow near the body apex, the new orthogonal curvilinear coordinates ξ, η are introduced in each meridional plane instead of r, θ by the following formulae:

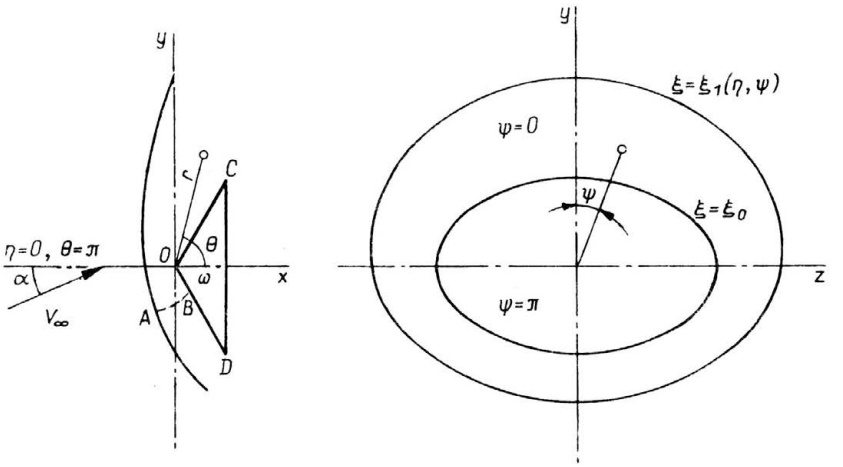

FIG. 1. Coordinate system.

(2.1) $$\xi = cr^n \sin n(\theta-\omega), \quad \eta = cr^n \cos n(\theta-\omega),$$

where $n = \pi/2(\pi-\omega)$, c is a certain scale factor.

At first we confine ourselves to the case of axisymmetrical bodies where ω (and also c) does not depend on the angle ψ. The equation $\xi = \xi_0(\xi_0 > 0)$ determines the surface of the cone-shaped body with the semi-angle ω and the apex bluntness having the curvature radius $R_0 = (1-n)^{-1}(\xi_0/c)^{1/n}$. If $\xi_0 = 0$, there is a sharp cone. This family of bodies includes cones ($\omega < \pi/2$), a flat-faced cylinder ($\omega = \pi/2$), bodies with cone-shaped concave noses ($\omega > \pi/2$). The line $\eta = 0$ ($\theta = \pi$) corresponds to the body axis continued into the shock layer.

As the basic sought functions we take three velocity components u, v, w along the ξ, η, ψ-directions, respectively, the pressure p and the density ϱ. All these functions are considered to be dimensionless assuming the critical sound velocity a_{cr} and the free stream density ϱ_∞ as the reference quantities.

The governing system of the problem includes the transformed continuity equation, the ξ- and ψ-momentum equations. To improve the computational properties of the solution in the vicinity of the body apex, these equations are multiplied by r^{n-2}. Carrying over to the right-hand side all the derivatives with respect to ψ, we represent the equations in such a divergence form

(2.2) $$\frac{\partial \tau u}{\partial \xi} + \frac{\partial \tau v}{\partial \eta} = P, \qquad \frac{\partial(\varrho u^2 + p)}{\partial \xi} + \frac{\partial \varrho uv}{\partial \eta} = Q,$$

$$\frac{\partial \varrho uw}{\partial \xi} + \frac{\partial \varrho vw}{\partial \eta} = T,$$

where

$$\tau = \left[\frac{\varkappa+1}{2\varkappa}\left(1 - \frac{\varkappa-1}{\varkappa+1}V^2\right)\right]^{1/(\varkappa-1)}, \qquad V^2 = u^2+v^2+w^2,$$

P, Q, T are the known functions of independent and dependent variables and contain naturally also the derivatives with respect to ψ.

The Bernoulli equation is used instead of the η -momentum equation

$$p = \frac{\varkappa+1}{2\varkappa}\left(1-\frac{\varkappa-1}{\varkappa+1}V^2\right)\varrho.$$

The equation of entropy conservation ($S = p/\varrho^{\varkappa}$) on a stream surface closes the governing system.

The system should be integrated in the region of mixed rotational flow between the body surface $\xi = \xi_0$ and the detached shock wave $\xi = \xi_1(\eta, \psi)$ which must be determined as the result of the solution. The normal velocity vanishes on the body (i.e. $u = 0$) and besides the entropy is here supposed to have the maximal value, i.e. the stagnation stream line AB on the windward plane $\psi = \pi$ (Fig. 1) passes across that point of the shock wave where the shock is normal. The following relation is satisfied at this point:

$$\operatorname{arctg}\frac{d\xi_1}{d\eta}+(n-1)(\omega-\theta)+\omega+\alpha = \frac{\pi}{2}.$$

The gasdynamical functions immediately behind the shock wave are calculated from the Rankine–Hugoniot relations. At the corner points of the body base (i.e. on the line CD), the longitudinal velocity component must have the sonic value, that is $v = 1$.

It should be noted that some terms in Eqs. (2.2) and in the boundary conditions have indeterminacies at the axis $\eta = 0$, which may be simply revealed.

3. Numerical method

The numerical solution of the problem is carried out by means of the method of integral relations, using the scheme of BELOTSERKOVSKII [10, 11] with polynomial approximations across the shock layer and trigonometrical approximations with respect to the meridional angle [12]. Equations (2.2) are integrated with respect to ξ from the body to the shock wave on a certain meridional plane $\psi = \psi_j = \text{const}$. For example, the integral relation for the first of these equations is derived as follows:

$$\frac{d}{d\eta}\int_{\xi_0}^{\xi_{1j}} \tau v\,d\xi-\tau_{1j}v_{1j}\frac{d\xi_{1j}}{d\eta}+\tau_{1j}u_{1j} = \int_{\xi_0}^{\xi_{1j}} P\,d\xi,$$

where the values of functions on the body and on the shock wave are denoted by the first index $i = 0$ and $i = 1$, respectively, while the second index j corresponds to the number of the meridional plane.

In the one-strip approximation, all the integrands in the integral relations are approximated linearly using their values on the body and on the shock wave. Then, in order to eliminate the independent variable ψ, the trigonometrical approximations are carried out. The meridional planes of interpolation $\psi = \psi_j = j\pi/2$ ($j = 0, 1, 2$) are taken and the following approximate representations

$$f_i = \frac{1}{2}(f_{i0}+f_{i2})+\frac{1}{2}(f_{i0}-f_{i2})\cos\psi,$$
$$w_i = w_{i1}\sin\psi \tag{3.1}$$

are assumed for all even functions f_i and odd functions w_i. Therefore the governing system (2.2) is reduced to the approximating system of ordinary differential equations with respect to η.

It should be noted that the interpolation (3.1) for even functions involves not three, but only two nodal meridional planes $\psi = 0$ and $\psi = \pi$. Such an approach proposed by KOZLOVA and MINAILOS [13] enables to decrease the number of the equations of the approximating system and to simplify the solution of the boundary value problem. The required values of even functions on the plane $\psi = \pi/2$ are found with the help of the interpolation (3.1).

The equations of the approximating system, which the two first equations (2.2) yield, are taken on the planes $\psi = 0$ and $\psi = \pi$. These equations for different values of ψ are interconnected only through the derivatives $(\partial w_i/\partial\psi)_j = (1-j)w_{i1}$ in P and Q (the last formula follows from the accepted interpolation for w). Actually, the symmetry conditions give for the other derivatives $(\partial f_i/\partial\psi)_j = 0$ and for the velocity component $w_{ij} = 0$ ($j = 0, 2$). As a result we obtain four approximating equations for four sought functions — the shock wave coordinate ξ_{1j} and the velocity on the body v_{0j}

$$\frac{d^2\xi_{1j}}{d\eta^2} = \Phi_j, \qquad \frac{dv_{0j}}{d\eta} = \frac{\Psi_j}{1-v_{0j}^2} \qquad (j = 0, 2). \tag{3.2}$$

To calculate the velocity component w_{01}, we shall not construct a corresponding integral relation but merely write the ψ-momentum equation on the body surface for $\psi = \pi/2$. The application of the trigonometrical interpolations (3.1) reduces it to the ordinary differential equation

$$\frac{dw_{01}}{d\eta} = \Omega_1. \tag{3.3}$$

Therefore the approximating system is closed. The concrete form of the system is presented in the work by CHUSHKIN [9]. The system becomes simpler in the case of two-dimensional flow about wedge at an angle of attack due to the absence of Eq. (3.3) and some terms in Φ_j and Ψ_j. More simplifications take place in the case of a zero angle of attack.

The approximating system (3.2)–(3.3) contains some terms with revealed indeterminacy at $\eta = 0$. Moreover, the derivatives $dv_{0j}/d\eta$ become infinite at the corner points of the body base C and D, where the velocity v_{0j} reaches the sonic value, i.e. $v_{0j} \to 1$. As for sharp bodies, the velocity derivative with respect to η at the tip is infinite for $\alpha \neq 0$, but it is finite for $\alpha = 0$.

One starts the integration of the approximating system from the axis $\eta = 0$, where in fact only three quantities are unknown, for instance ξ_{10}, $d\xi_{10}/d\eta$, v_{00}, since here the following evident relations exist:

$$v_{00} = -v_{02} = -w_{01}, \qquad \xi_{10} = \xi_{12}, \qquad \frac{d\xi_{10}}{d\eta} = -\frac{d\xi_{12}}{d\eta}.$$

Three these unknown quantities are determined as a result of the solution of the boundary-value problem satisfying the sonic velocity condition at two corner points of the body base C and D ($v_{00} = v_{02} = 1$) and the condition that the stagnation stream line

AB passes across the normal shock. The stagnation stream line can be traced by integrating the appropriate differential equation. For the zero angle of attack, the stagnation point is located at the body apex; thus here the last condition is automatically satisfied and $v_{00} = d\xi_{10}/d\eta = 0$ at $\eta = 0$. If the body length (that is the position of the body base) is not given, an arbitrary value ξ_{10} at $\eta = 0$ may be chosen. When the systematical calculations are carried out, the typical run of time required for the solution of the boundary value problem with three unknown parameters is rather short since, for instance, the sought parameter ξ_{10} appears to depend on α very weakly.

4. Some results of computations

The developed method is used for the numerical investigation of flows about axisymmetrical cone-shaped bodies located in a supersonic free stream at an angle of attack. The bodies have a finite length, a small apex bluntness and a semi-angle ω greater than its limiting value ω_{lim}. The parameters are chosen within the following intervals: $\omega = 60°-120°$, $\xi_0 = 0.001-0.1$, $M_\infty = 2-\infty$, $\alpha = 0°-25°$, the specific heat ratio is $\varkappa = 1.4$. The accuracy of the calculated solutions was estimated by comparison with other numerical solutions and experiments only in the case of a zero angle of attack, as such data at $\alpha \neq 0$ were not available for us. It is proved that the accuracy of the prediction is sufficient for the general analysis of shock wave features and body distributions of gasdynamical functions, though it diminishes for smaller free stream Mach numbers and larger angles of attack.

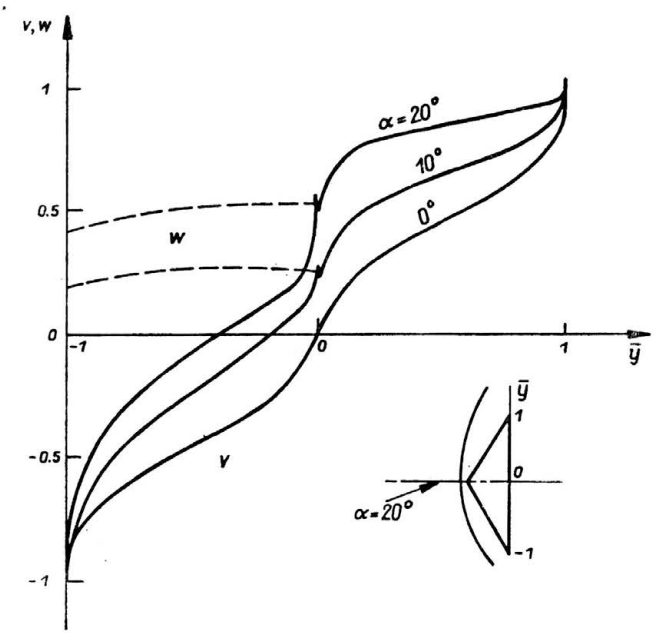

FIG. 2. Distributions of longitudinal v and circumferential w velocities along conical body $\omega = 60°$ for various angles of attack α, $M_\infty = 3$.

Now let us discuss a number of new computational results which supplement the earlier publication [9]. At first, in Figs. 2–4 we present some numerical data for the flow about a conical body with $\omega = 60°$, $\xi_0 = 0.01$ at the free stream Mach number $M_\infty = 3$ and various angles of attack. The apex curvature radius of this body is 0.52% of its length.

Figure 2 demonstrates the behaviour of the longitudinal velocity v along the body

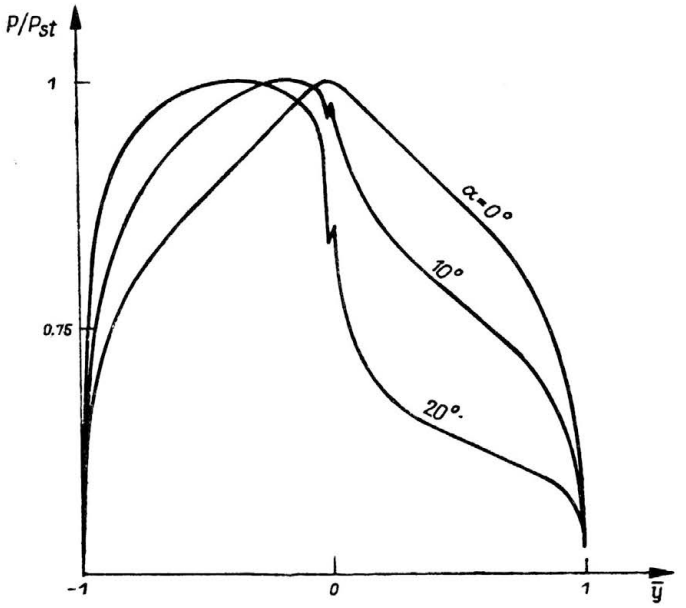

FIG. 3. Pressure distribution along conical body $\omega = 60°$ for various angles of attack α, $M_\infty = 3$.

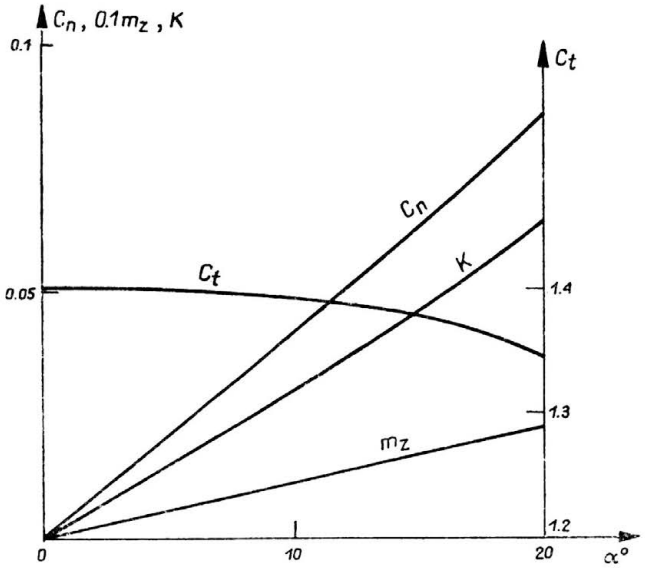

FIG. 4. Aerodynamical coefficients versus angle of attack α for conical body $\omega = 60°$, $M_\infty = 3$.

surface. It is given as the function of the relative ordinate $\bar{y} = y/y_C$, where y_C is the distance of the body corner point C from the axis $\eta = 0$. The right and the left parts of the graph correspond to the leeward ($\varphi = 0$) and the windward ($\varphi = \pi$) sides, respectively. When the angle of attack increases, the velocity v changes rapidly in the vicinity of the small bluntness and may exceed the sonic value at very large angles α. As it is seen, a small portion of nonmonotonic variation of v occurs on the leeward side at $\alpha \neq 0$. The circumferential velocity w, which is a feature of three-dimensional flows, is plotted by the dashed line for the body generator $\varphi = \pi/2$. This function changes more smoothly.

The corresponding body distribution of the pressure p/p_{st} (related to the stagnation pressure p_{st}) is shown in Fig. 3. When the angle of attack increases and the flow direction on the leeward side of the body approaches the local limiting angle, the pressure and velocity distributions are transformed and tend to flatten out in a region behind the bluntness.

The shock wave on the symmetry plane is also drawn in Fig. 2 for the same conical body at $\alpha = 20°$. When the angle of attack changes, the shock wave accordingly rotates, weakly alternating its shape. The stagnation point is removed from the body apex almost linearly versus α.

The coefficients of tangential force C_t, of normal force C_n and of longitudinal moment m_z with respect to the axis passing through the body apex and also the ratio $K = C_n/C_t$ are plotted versus α in Fig. 4. All the coefficients are referred to the body base area and m_z is additionally referred to the body length. The coefficient C_t slightly diminishes with the increase of α, as the pressure on the leeward side drops larger than it grows on the

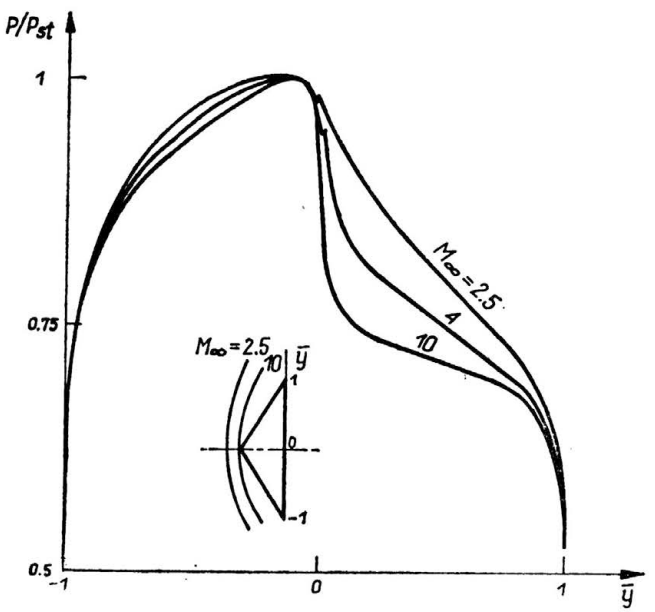

FIG. 5. Pressure distribution along conical body $\omega = 60°$ for various free stream Mach numbers M_∞, $\alpha = 10°$.

windward side. The dependences $C_n = C_n(\alpha)$ and $m_z = m_z(\alpha)$ are almost linear within the considered interval of α.

Two next graphs illustrate the dependences of some flow properties on the free stream Mach number M_∞. Here the data are presented for the same conical body with $\omega = 60°$, $\xi_0 = 0.01$ at the angle of attack $\alpha = 10°$. The pressure distribution on the leeward and windward sides of the body and the form of the shock wave on the symmetry plane of the flow are shown in Fig. 5. When the free stream Mach number M_∞ grows, pressure gradients in the vicinity of the bluntness increase strongly and, further, the pressure distribution on the leeward side tends to flatten out. This is inherent in flow regimes close to limiting ones.

The shock wave detachment distance Δ (related to the radius of the base) at the axis $\eta = 0$, the velocity component v_0 at the front point of the body and the relative ordinate of the stagnation point $\bar{y}_{st} = y_{st}/y_C$ are given in Fig. 6 as the functions of the free stream Mach number M_∞ and velocity $\lambda_\infty = V_\infty/a_{cr}$.

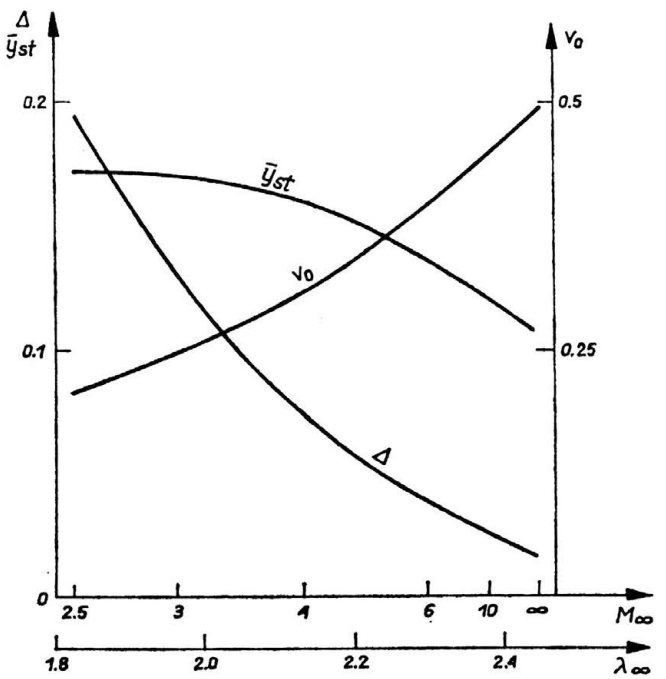

FIG. 6. Shock wave detachment distance Δ, stagnation point coordinate $\bar{y}_{st}$ and velocity at apex v_0 versus M_∞ for conical body $\omega = 60°$, $\alpha = 10°$.

Now we study the influence of the semi-angle ω of cone-shaped bodies. Figures 7 and 8 correspond to the bodies with $\xi_0 = 0.01$, located in the free stream at the angle of attack $\alpha = 10°$ and the Mach number $M_\infty = 3$. Here the shock waves on the symmetry plane and the stagnation stream lines are drawn for the cones $\omega = 60°$, $75°$, the flat-faced cylinder $\omega = 90°$ and the body with a cone-shaped concave nose $\omega = 105°$. The distributions of the velocity components v and w are also depicted for this family of bodies. It is in-

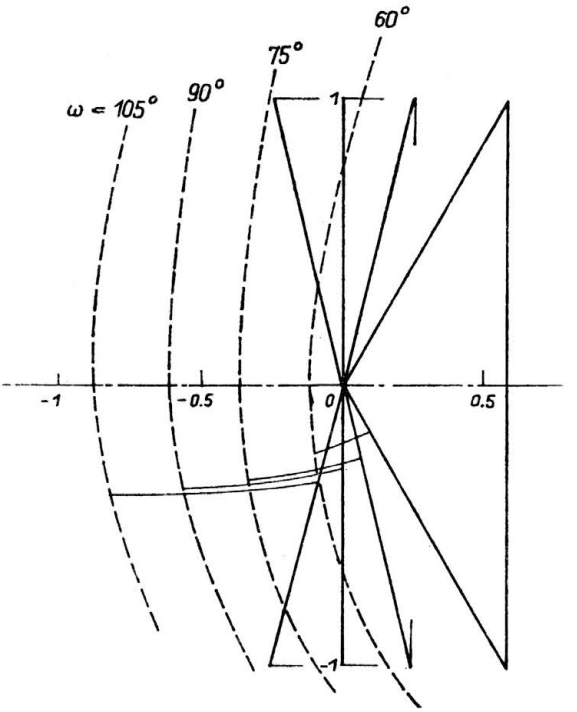

FIG. 7. Shock waves for conical bodies with various apex semi-angles ω, $M_\infty = 3$, $\alpha = 10°$.

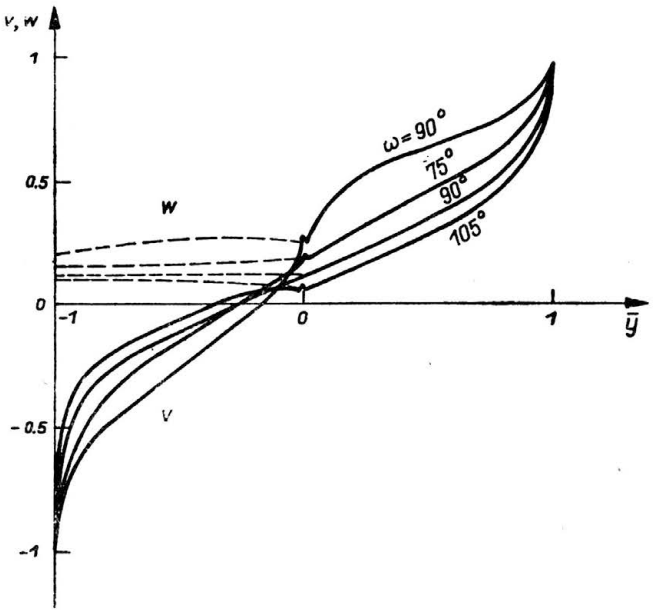

FIG. 8. Distributions of longitudinal v and circumferential w velocities along various conical bodies, $M_\infty = 3$, $\alpha = 10°$.

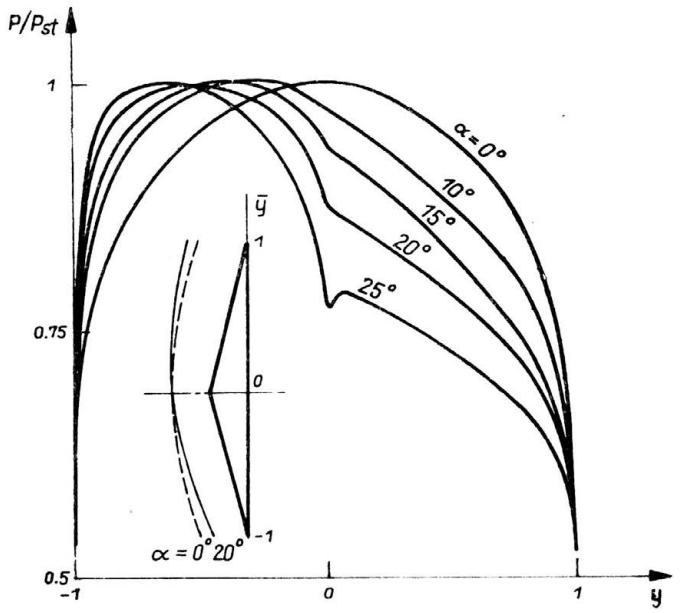

FIG. 9. Pressure distribution along conical body $\omega = 75°$ for various angles of attack α, $M_\infty = 4$.

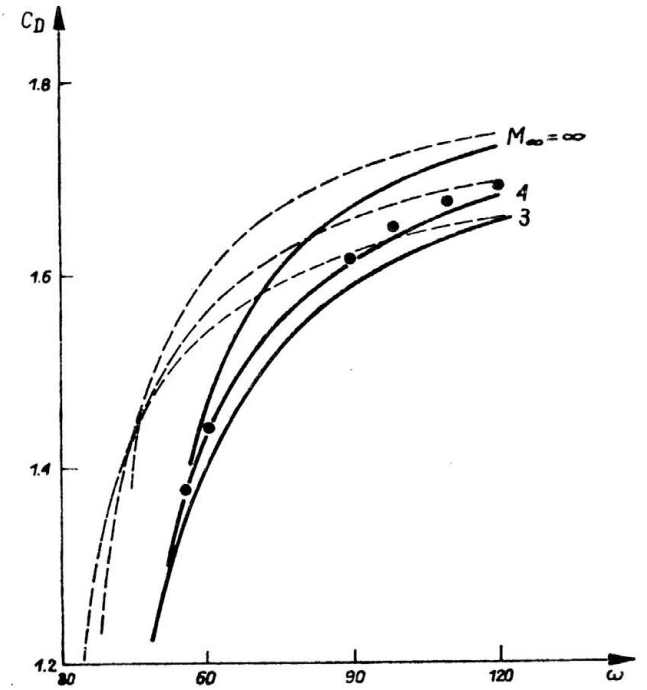

FIG. 10. Drag coefficient for sharp cones (solid line) and wedges (dashed line) for various apex semi-angles ω and free-stream Mach numbers M_∞, $\alpha = 0°$. Comparison with experiment (dark circle).

teresting to note that a small region of nonmonotonic variation of v is located on the leeward side for a convex nose and on the windward side for a concave nose (it is naturally absent for a flat nose).

The pressure distribution for the conical body $\omega = 75°$, $\xi_0 = 0.1$ at $M_\infty = 4$ and $\alpha = 10°$ is given in Fig. 9. Comparison of this graph with Fig. 3 indicates that the pressure and, accordingly, the velocity change less abruptly on blunter cones.

Let us present a graph from the work [7]. In Fig. 10 the drag coefficient C_D for sharp cones (solid line) and wedges (dashed line) is plotted versus the body semi-angle ω at various M_∞ and $\alpha = 0°$. It is interesting to observe that within the considered interval of M_∞, the drag coefficient of the sharp cone with the semi-angle ω tending to the limiting value ω_{lim} for a flow regime with a detached shock wave proves to be 11–13% less than for a flow regime with an attached conical shock wave at $\omega = \omega_{\text{lim}}$. This results from the fact that in the first case higher pressure in the vicinity of the cone tip acts on a small area, while the main contribution into C_D is due to the drop of pressure to the sonic value at the corner point of the base (in comparison with the constant pressure on the cone with $\omega = \omega_{\text{lim}}$ in the second case). The effect obtained qualitatively remains as ω increases within 10°–20° or α slightly deviates from zero. This effect and also the sufficiently good accuracy of the numerical results were later confirmed by the experimental data of AMARANTOVA *et al.* [14] at $M_\infty = 4.03$ and $\alpha = 0°$, shown by black circles in Fig. 10. An analogous effect is not observed in the calculated flows about wedges.

5. Bodies with elliptical cross-section

Now we discuss the extension of the numerical technique worked out to cone-shaped bodies with a noncircular, elliptical cross-section in the case, where the free stream velocity vector is parallel to the symmetry plane of the body. Here, in contradistinction to an axisymmetrical body, a semi-angle of the body ω is not constant, but a given function of the meridional angle ψ. As before, the problem is solved using the coordinates ξ, η, ψ. The two first coordinates are defined by the same expression (2.1), but now with $\omega = \omega(\psi)$ and $n = n(\psi)$. The scale factor c is also a function of ψ which is chosen in accordance with the shape of the body cross-section and is supposed to satisfy the symmetry conditions $dc/d\psi = 0$ at $\psi = 0, \pi/2, \pi$.

Solving the problem, only three meridional planes $\psi = 0$, $\pi/2$ and π are considered where the coordinates ξ, η, ψ are orthogonal (though they are not orthogonal at other arbitrary values of ψ). Therefore the approximating system for conical bodies with an elliptical cross-section will differ from the system (3.2)–(3.3) only owing to the fact that the body semi-angle ω and the scale factor c at $\psi = \pi/2$ are other than at $\psi = 0$ and $\psi = \pi$.

Since the trigonometrical approximations of the type (3.1) only with one or two interpolation nodes are employed, it appears reasonable to modify them in order to take into account better the elliptical shape of the body cross-section. Thus the meridional angle ψ in the approximations (3.1) is replaced by the corresponding elliptical variable denoted,

say, through χ. For the ellipse with a relative thickness t, the variables ψ and χ are connected by the easy relation

$$\operatorname{tg}\chi = t\operatorname{tg}\psi.$$

A higher accuracy of solution for conical bodies with an elliptical cross-section may be obtained if one adds another interpolation node on the plane $\psi = \pi/2$ and an appropriate term in the first interpolation polynomial (3.1). Then, operating with two first equations of the system (2.1), two new integral relations are written for this meridional plane, which are reduced to two additional approximating equations of view (3.2) for ξ_{11} and v_{01}. The fourth unknown quantity — the value of the shock wave derivative $d\xi_{11}/d\eta$ appears in the boundary conditions at $\eta = 0$. To specify this quantity, one must use the condition of regularity at the singular point arisen in the equation for v_{01} in the transonic region.

Recently we have performed some test calculations of three-dimensional flows about conical bodies with elliptical cross-section. The flow regime with a detached shock wave was studied. A computed example is presented in Fig. 11 where the bodies with various

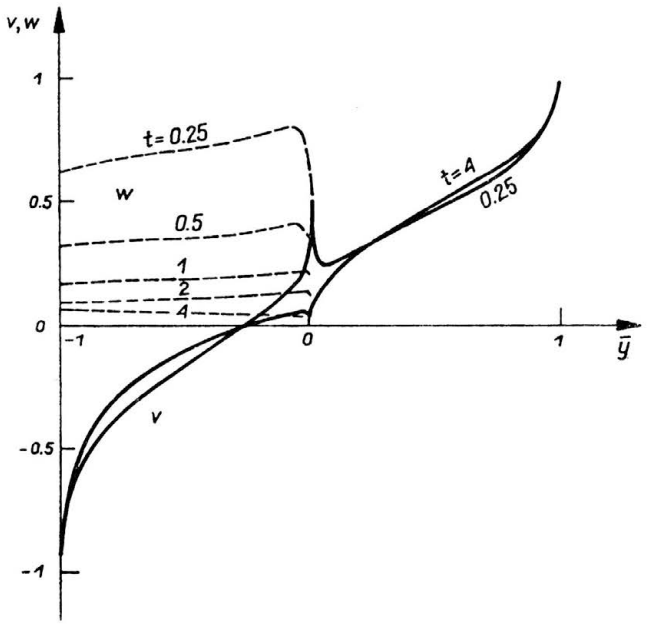

FIG. 11. Velocity distribution along conical bodies with elliptical cross-section and various relative thicknesses t, $M_\infty = 4$, $\alpha = 10°$.

relative thicknesses t are considered. The bodies have the same finite length, the small spherical apex bluntness ($\xi_0 = 0.01$), the same semi-angle $\omega = 75°$ at $\psi = 0$ and $\psi = \pi$ and the different corresponding semi-angle $\omega_1 = \operatorname{arctg}(t^{-1}\operatorname{tg}\omega)$ at $\psi = \pi/2$. The results are given for the free stream Mach number $M_\infty = 4$, the angle of attack $\alpha = 10°$ and the specific heat ratio $\varkappa = 1.4$. The distributions of the longitudinal velocity v on the body leeward and windward sides and of the circumferential velocity w at $\psi = \pi/2$ are plotted in the graph.

Concluding, it should be remarked that the developed numerical technique may be simply extended to the case of a real gas with high temperature equilibrium physical-chemical processes.

References

1. Г. П. Воскресенский, П. И. Чушкин, *Численные методы расчета сверхзвукового обтекания тел под углом атаки*, Успехи механики, **3**, 2, 47–95, 1980.
2. В. Н. Иванова, Ю. Б. Радвогин, *Численный метод расчета трехмерных обтеканий головной части заостренных тел с отошедшей ударной волной*, Москва, Ин-т прикл. мат. им. М. В. Келдыша АН СССР, препринт № 126, 1980.
3. В. Н. Иванова, Ю. Б. Радвогин, *Численное исследование трехмерного обтекания заостренных тел с отошедшей ударной волной*, Москва, Ин-т прикл. мат. им. М. В. Келдыша АН СССР, препринт № 28, 1981.
4. К. И. Бабенко, Г. П. Воскресенский, *Численный метод расчета пространственного обтекания тел сверхзвуковым потоком газа*, Ж. вычисл. мат. и мат.физ., **1**, 6, 1051–1060, 1961.
5. В. М. Ковеня, Г. А. Тарнавский, Н. Н. Яненко, *Неявная разностная схема для численного решения пространственных уравнений газовой динамики*, Ж. вычисл. мат. и мат. физ., **20**, 6, 1465–1482, 1980.
6. А. А. Дородницын, *Об одном методе численного решения некоторых нелинейных задач аэрогидродинамики*, Труды 3-го Всесоюзн. мат. съезда, 1956; Москва, АН СССР, т. 3. 447–453, 1958.
7. П. И. Чушкин, *Отошедшая ударная волна перед клином или конусом*, Ж. вычисл. мат. и мат. физ., **14**, 6, 1600–1605, 1974.
8. П. И. Чушкин, *Клин с малым затуплением в сверхзвуковом потоке под углом атаки*, Докл. АН СССР, **241**, 6, 1296–1299, 1978.
9. П. И. Чушкин, *Конус с малым затуплением в сверхзвуковом потоке под углом атаки*, Ж. вычисл. мат. и мат. физ., **20**, 6, 1525–1535, 1980.
10. О. М. Белоцерковский, *Обтекание кругового цилиндра с отошедшей ударной волной*. Докл. АН СССР, **113**, 3, 509–519, 1957.
11. О. М. Белоцерковский, *О расчете обтекания осесимметричных тел с отошедшей ударной волной на электронной счетной машине*, Прикл. мат. и мех., **24**, 3, 511–517, 1960.
12. О. М. Белоцерковский, П. И. Чушкин, *Численный метод интегральных соотношений*, Ж. вычисл. мат. и мат. физ., **2**, 5, 731–759, 1962.
13. И. Г. Козлова, А. Н. Минайлос, *Несимметричное обтекание лобовой части тела вращения сверхзвуковым потоком совершенного газа*, Ж. вычисл. мат. и мат. физ., **7**, 3, 594–608, 1967.
14. И. И. Амарантова, В. Г. Буковшин, В. И. Шустов, *Экспериментальное исследование обтекания острых конусов с околокритическими и закритическими углами раствора*, Изв. АН СССР. Мех. жидк. и газа, 2, 195–198, 1978.

USSR ACADEMY OF SCIENCES,
COMPUTING CENTRE, MOSCOW, USSR.

Received September 14, 1983.